Epistasis and cryptic QTL identified using modified bulk segregant analysis of copper resistance in budding yeast

Cassandra Buzby[1,2], Yevgeniy Plavskin[1,2], Federica M.O. Sartori[1,2,3], Qiange Tong[1,2], Janessa K. Vail[1,2], Mark L. Siegal[1,2*]

[1] Department of Biology, New York University, New York, NY, USA

[2] Center for Genomics and Systems Biology, New York University, New York, NY, USA

[3] Current affiliation: Department of Oncological Sciences, Mount Sinai, New York, NY, USA

* Corresponding author

E-mail: mark.siegal@nyu.edu (MLS)

Abstract

The contributions of genetic interactions to natural trait variation are challenging to estimate experimentally, as current approaches for detecting epistasis are often underpowered. Powerful mapping approaches such as bulk segregant analysis, wherein individuals with extreme phenotypes are pooled for genotyping, obscure epistasis by averaging over genotype combinations. To accurately characterize and quantify epistasis underlying natural trait variation, we have engineered strains of the budding yeast *Saccharomyces cerevisiae* to enable crosses where one parent's chromosome is fixed while the rest of the chromosomes segregate. These crosses allow us to use bulk segregant analysis to identify quantitative trait loci (QTL) whose effects depend on alleles on the fixed parental chromosome, indicating a genetic interaction with that chromosome. Our method, which we term epic-QTL (for *epi*static-with-*c*hromosome *QTL*) analysis, can thus identify interaction loci with high statistical power. Here we perform epic-QTL analysis of copper resistance with chromosome I or VIII fixed in a cross between divergent naturally derived strains. We find seven loci that interact significantly with chromosome VIII and none that interact with chromosome I, the smallest of the 16 budding yeast chromosomes. Each of the seven interactions alters the magnitude, rather than the direction, of an additive QTL effect. We also show that fixation of one source of variation — in this case chromosome VIII, which contains the large-effect QTL mapping to *CUP1* — increases power to detect the contributions of other loci to trait differences.

Author Summary

Most traits of interest that vary in populations are determined by multiple genetic factors, as well as by environmental variation and random chance. These influences may combine in complicated ways, for example when the effect of one genetic variant depends on genetic variants elsewhere in the genome. Such dependencies are difficult to identify and characterize because testing many possible combinations of influences reduces statistical power. We address this challenge by combining bulk segregant analysis, a robust method for detecting effects of individual genetic variants averaged across genetic backgrounds, with chromosome fixation in budding yeast. This approach allows us to detect gene-variant effects that depend on the fixed chromosome with statistical power comparable to that achieved when detecting background-independent effects. Applying the approach to copper sulfate resistance, we identify and characterize interaction effects and, by removing one source of variation (a single yeast chromosome), improve detection of background-independent effects as well.

Introduction

Predicting phenotype from genotype is a central goal of genetics research, yet even with great advances in sequencing technology and experimental scale, accurate characterization of how genetic differences translate into trait differences remains elusive. Many genetic influences are subtle, and most traits of interest that vary in populations are determined by multiple genetic factors, as well as by environmental variation and random chance [1–4]. Moreover, these influences may combine in

68 complicated ways, for example in the form of gene-by-gene (epistatic) or gene-by-
69 environment interactions [5–7].

70 Epistasis is particularly challenging to detect in standard quantitative-genetic
71 analyses because the number of possible interaction effects vastly exceeds the number
72 of single-locus (additive) effects, leading to very low statistical power to detect the
73 interactions [5]. Standard analyses fit additive effects before interaction effects, which
74 can lead to the mistaken inference that epistasis is less salient than it actually is [8,9]. If
75 interacting alleles are rare in a mapping population, under-detection of epistasis is even
76 more severe. Failure to detect epistasis in turn compromises accurate prediction of an
77 individual's phenotype from genotype, even when an additive model appears to fit well
78 [8–10].

79 The distribution of types of epistatic effects influences both detection of loci with
80 effects on traits and evolutionary trajectories [11–13]. Magnitude epistasis changes the
81 size of an allele's effect without changing its direction (beneficial vs. detrimental),
82 whereas sign epistasis changes the direction. Sign epistasis gives rise to peaks and
83 valleys in fitness landscapes and can alter the order of mutations that increase fitness
84 [11]. Models of distribution and patterns of these effects have been postulated, with two
85 extremes being global epistasis and idiosyncratic epistasis. Global epistasis indicates
86 underlying predictability of the effects of individual alleles, perhaps based on a latent
87 phenotype such as protein stability or physiological health [14,15]. Idiosyncratic
88 epistasis, by contrast, refers to unpredictable allele effects that ultimately depend on
89 details of particular alleles [16,17]. Data on the relative prevalences of magnitude and
90 sign epistasis, which are currently lacking, would inform which model of epistasis

91 patterns is more suitable, which in turn will inform models of the evolution of complex
92 traits.

93 An ideal method for identifying and characterizing epistatic contributions to trait
94 variation would have equal (and high) statistical power to detect additive and interaction
95 effects. Experimental designs with extremely large sample sizes are now common [18–
96 22], but the most powerful of these favor (or exclusively detect) additive effects. One
97 such experimental design is bulk segregant analysis (BSA). In a typical BSA
98 experiment, many progeny are produced from a cross between divergent parental
99 genotypes, progeny with extreme values of a trait of interest are pooled, and high-
100 coverage genome sequencing is used to detect loci at which the allele frequency in the
101 selected bulk deviates significantly from the allele frequency in an unselected (or
102 oppositely selected) bulk [18,23]. Although BSA benefits from sampling many
103 individuals — over 10 million in some cases [18] — it cannot detect genetic interaction
104 effects because pooled sequencing results in an estimate of the effect of any one locus
105 that is the average across all genotypes at other loci.

106 Genotyping and phenotyping individuals rather than pools avoids the averaging
107 issue, but suffers from the problem that potential pairwise interactions far outnumber
108 additive effects of single loci, resulting in greatly reduced statistical power. Two recent
109 attempts to detect epistasis using very large sample sizes illustrate this challenge. One
110 study, which genotyped ~200,000 diploid progeny of a yeast cross, identified numerous
111 interaction effects, but found a strong positive correlation between the additive effect of
112 a locus and the number of pairwise interactions it participates in [22]. This correlation
113 could reflect the true distribution of epistatic effects or an influence of additive-effect size

114 on detectability of interactions [22]. Another study genotyped ~100,000 haploid
115 segregants but to maximize power tested only interactions between pairs of additive-
116 effect QTL [21]. This study found evidence of epistatic effects, but found the additive-
117 plus-pairwise model to have only modest predictive power for the phenotypes of
118 reconstructed genotypes, suggesting that effects remain undetected [21]. Another
119 recent study did not genotype large numbers of segregants, but instead engineered
120 naturally occurring gene variants into four divergent yeast strains to detect genetic
121 background-dependent effects on growth. This study found a substantial fraction of
122 variants to have background-dependent effects, but was limited to variants in and
123 around 103 genes previously shown to be interaction hubs in genome-wide double-
124 mutant screens [24,25]. The results of these studies suggest that unbiased approaches
125 are needed that equalize the power to detect additive and epistatic effects.

126 To identify and characterize genetic interactions with comparable statistical
127 power to that of additive effects, we combine chromosome substitution with BSA in the
128 genetically tractable budding yeast, *Saccharomyces cerevisiae*. We call this method
129 epic-QTL (for *epi*static-with-*c*hromosome *QTL*) analysis. To perform epic-QTL, we cross
130 two divergent natural isolates of *S. cerevisiae*, but before generating segregating F2
131 progeny from the resulting F1 diploid, we first eliminate one chromosome from one
132 parent, fixing the remaining homologous chromosome. The result is that all surviving F2
133 haploids contain identical copies of one chromosome, but have unique combinations of
134 the two parents' alleles on all other chromosomes. We also perform the reciprocal
135 cross, in which the other parent's chromosome is fixed. We then grow the haploid
136 progeny in selective or non-selective conditions. Here, we use the presence or absence

137 of copper (II) sulfate ($CuSO_4$) as a selective condition, with the presence of copper and
138 subsequent oxidative stress selecting for individuals with alleles that promote survival in
139 this environment. Standard BSA would compare the allele frequencies in bulks grown in
140 the presence or absence of copper to identify additive QTL for the trait of copper
141 resistance. In epic-QTL, there are four bulks rather than two. By comparing the QTL
142 identified in the crosses with the reciprocal fixed chromosomes, we can identify loci
143 whose effects differ between genetic backgrounds. The loci that are dependent on
144 parental-chromosome background for their effect are thus epistatic with that fixed
145 chromosome and are detected with statistical power usually only afforded to additive
146 effects. In practice, this comparison is done by including a parental-chromosome (or
147 genetic-background) term in a logistic-regression model that is fit to the data from all
148 four bulks simultaneously. An additional benefit of chromosome substitution is an
149 increase in power for detection of additive effects by removing a source of variance in a
150 population. With only one cross, the fixation of a chromosome containing a major QTL
151 allows the remaining segregating sites to exert greater influence over membership in
152 the selected bulk.

153 Using epic-QTL we can determine where QTL that interact with each fixed
154 chromosome lie relative to where additive QTL lie, and how prevalent interactions are
155 for a given trait, in this case copper sulfate resistance. We focus on copper sulfate for
156 three reasons: 1) its extensive use in prior *S. cerevisiae* studies, allowing comparison
157 with previous results; 2) the potential for unexplained heritability, in that copper
158 resistance shows a large gap in broad and narrow sense heritability compared to other
159 traits [4]; and 3) its ecological and physiological relevance [26–28]. In addition, one

160 major interaction hub identified by Matsui *et al.* was *CUP1* on chromosome VIII, which is
161 a major driver of copper resistance, and thus a perfect candidate for chromosome
162 fixation [22]. We fixed chromosomes I or VIII in a cross between strains derived from an
163 oak tree or from a wine barrel, which differ on average at 1 in 200 base pairs [29]. The
164 variants in these strains reflect natural genetic diversity, offering insights into genetic
165 interactions that might occur within populations. We demonstrate that this method can
166 be used to remove sources of trait variation to reveal additive QTL otherwise
167 undetected at this experimental scale, as well as to identify interaction QTL with high
168 statistical power. We find that these interactions often occur within significant additive
169 QTL peaks, providing evidence of a lack of pervasive sign epistasis.

170

171 Results

172

173 Implementation of epic-QTL for copper resistance

174 Our method to identify QTL interacting with a fixed chromosome, or epic-QTL,
175 combines chromosome substitution with BSA in a cross of two parental yeast strains.
176 For the parental strains we used divergent natural isolates of *S. cerevisiae*: NCYC3631
177 and NCYC3591 (hereafter “Oak” and “Wine”, respectively). Before crossing the two
178 strains, we engineered one strain of each parent to contain the inducible *GAL1*
179 promoter (*pGAL1*) adjacent to the centromere of one chromosome. Inducing a high
180 level of transcription through the centromere destabilizes the kinetochore, resulting in
181 missegregation of the chromosome during mitosis so that a strain with only the

182 homologous chromosome remaining can be isolated [30]. By this method, we fixed
183 chromosome I in each background (Fig 1A) and, separately, chromosome VIII in each
184 background (Fig 1B). We then mated the Wine *pGAL1* strain with the Oak non-*pGAL1*
185 strain (Fig 1C), and vice versa, to produce diploids with reciprocal conditional
186 chromosomes. Each diploid strain was then plated on galactose to induce *pGAL1*. After
187 re-plating colonies from the galactose-containing media to ensure clonality, individual
188 colonies were checked by Sanger sequencing at biallelic regions to confirm loss of the
189 conditional chromosome. Each of these aneuploid (2N–1) strains was then sporulated
190 to produce an F2 population of haploid segregants fixed for a single parent's
191 chromosome (Fig 1C), which could then be used for BSA (Fig 1D).
192
193 **Fig 1. Insertion of *GAL1* promoter allows for fixed chromosomes.** (A–B) Matings to
194 produce reciprocal diploids with single conditional chromosomes for chromosome I (A)
195 and chromosome VIII (B). (C) Induction of the *GAL1* promoter adjacent to the
196 centromere destabilizes the chromosome's kinetochore, leading to loss of that
197 chromosome in diploids and fixation of the homologous chromosome in F2 haploid
198 progeny. One representative cross of the four (Oak I) is shown. (D) BSA experiment for
199 interactions with chromosome I, allowing detection of additive effects by comparison of
200 selected (blue) and unselected (white) bulks and of interactions with chromosome I
201 background (orange or purple). One representative haploid segregant is shown beneath
202 each bulk's flask.
203

204 Before proceeding to BSA, we demonstrated that the Oak and Wine parental
205 strains, which have been shown to differ phenotypically in multiple traits [31,32], differ in
206 the phenotype of copper sulfate resistance. We grew populations of haploids of each
207 parental strain in an array of doses of $CuSO_4$ in rich media (YPD), and compared the
208 cell counts of each population to a control of the same seed culture. The Wine haploid
209 strain showed higher resistance to $CuSO_4$, surviving at almost double the percentage at
210 which the Oak haploid strain survived in mid-range doses of $CuSO_4$ (S1 Fig).
211 Due to chromosome fixation, the relative intensity of selection varied at the same
212 doses of $CuSO_4$ between crosses. Specifically, as shown below, Wine chromosome VIII
213 has a strongly advantageous allele, so the same dose of $CuSO_4$ produces more
214 survivors in the Wine VIII cross than in the Oak VIII cross. We therefore tested multiple
215 doses of $CuSO_4$ to determine the dose that produced 1–10% survival of the population.
216 This range of selection optimizes BSA by balancing detectable effects and retention of
217 causative genetic variation in the surviving population [33]. Unselected bulks from each
218 cross were seeded in YPD at 10% the cell number at which selected bulks were seeded
219 so that their final cell densities were approximately the same as those in the selected
220 bulks.
221

222 Known drivers of resistance are identified as additive QTL

223 Previous studies have identified additive QTL for the trait of copper sulfate
224 resistance in a variety of *S. cerevisiae* strains [2,4,18,34]. In addition, multiple studies
225 have identified mechanistic drivers of copper resistance, including certain alleles of the
226 *FRE1* gene and copy number amplification of the *CUP1* locus [27,35,36]. Because there

227 is overlap across strains for identification of some QTL [37], one form of validation of
228 epic-QTL would be for previously known resistance loci to be detected by epic-QTL as
229 additive effects (that is, effects that do not depend on the parental origin of the fixed
230 chromosome).

231 In epic-QTL, as in standard BSA, allele frequency differences between bulks at a
232 given genomic site indicate a contribution of variation at that site to bulk membership.
233 For the reciprocal chromosome I crosses and, separately, for the reciprocal
234 chromosome VIII crosses, we sequenced the four bulks (selected vs. unselected for
235 each Oak or Wine fixed chromosome) at high depth of coverage (average ~70X per site
236 per bulk) to estimate allele frequencies. We partitioned the effects of selection, parental-
237 chromosome background (hereafter "background"), and their interaction using a logistic
238 regression model as described in *Materials and Methods*. The selection term's
239 coefficient reflects the additive effect on $CuSO_4$ survival regardless of parental-
240 chromosome background, whereas the interaction term reflects epistasis with the fixed
241 chromosome. To visualize significant effects across the genome, we use the z-score of
242 each coefficient. The z-score is advantageous over the parametric *p*-value to which it
243 corresponds because its sign indicates the direction of effect of the fixed chromosome,
244 and because we use permutations of it to determine a threshold of false discovery rate,
245 detailed in *Materials and Methods*. To compare significance regardless of effect
246 direction, the majority of plots display absolute values of z-scores. Signed z-scores for
247 each coefficient and position are included in supplemental data (S1 Table).

248 The additive (selection) peaks on chromosomes VIII and XII are very close to the
249 known copper-resistance genes, *CUP1* and *FRE1*, respectively (Fig 2). These genes

250 are well documented to play critical roles in copper detoxification mechanisms in yeast.
251 *CUP1* encodes a metallothionein involved in sequestering copper ions, thereby
252 mitigating copper toxicity within the cell [38]. *FRE1* encodes a ferric reductase enzyme
253 that contributes to iron uptake and detoxification of copper [39,40]. In both fixed-
254 chromosome backgrounds, we identify *FRE1* as a major driver of resistance, with peak
255 maxima <6 kb away from the coding region (Fig 2). The crosses for the two fixed-
256 chromosome backgrounds are independent, so the agreement between the two crosses
257 further validates the method. In the strains fixed for chromosome I, the peak on
258 chromosome VIII is upstream of the *CUP1* coding sequence. *CUP1* has two paralogs,
259 *CUP1-1* and *CUP1-2*, within a larger tandemly duplicated region in the reference
260 genome of the laboratory strain S288C. We found that the region surrounding these
261 paralogs had poor mapping quality, likely due to repetitive sequences and potential
262 *CUP1* copy variation, which is a known mechanism of resistance [38]. These regions
263 were therefore excluded from our variant calling, and so the peak upstream of the
264 coding sequence is as close as can be to this known driver of copper resistance.
265
266 **Fig 2. Known drivers of copper resistance identified as additive QTL**. Traces
267 represent absolute z-scores of additive (selection) coefficients on chromosomes VIII
268 and XII, as indicated. Dashed line corresponds to the experiment with chromosome I
269 fixed and solid line corresponds to the experiment with chromosome VIII fixed.
270 Horizontal lines indicate the 5% false discovery rate (FDR) threshold for each
271 experiment. Turquoise vertical lines represent the locations of CUP1 and FRE1, both of
272 which fall under large-effect additive peaks as expected.

Fixing Large Effect QTL Increases Power for Detection of Additive Effects

The resolution and reproducibility of epic-QTL are further supported by additive QTL that do not map to known copper-resistance loci. Between the experiment with fixed chromosome I and the experiment with fixed chromosome VIII, we identified many overlapping selection-QTL peaks with locations of highest absolute z-scores within 1.5 kb of one another, indicating not only that there is high resolution and reproducibility but also that the underlying mechanisms of resistance do not strongly differ in the presence of one or the other fixed chromosome (Fig 3, S2 Table).

Fig 3. Consistent additive peaks identified in each fixed parental-chromosome experiment. Additive effects for the experiment with chromosome I fixed (dashed lines) and the experiment with chromosome VIII fixed (solid lines), shown as the absolute value of the selection coefficient's z-score, with 5% FDR thresholds shown as horizontal lines of the same type. The only trace for chromosome I is solid, and the only trace for chromosome VIII is dashed, because of the fixed chromosome in each experiment. Peaks for each experiment are denoted as points on the traces as well as vertical lines below (fixed chromosome I as light blue, top strip, and fixed chromosome VIII as dark blue, bottom strip). In these strips, regions of significant z-scores are shown in gray, with intensities proportional to absolute z-score.

295 Having established that our method identifies additive QTL, we next investigated
296 the result of chromosome fixation on additive effects. Removal of a major-effect QTL is
297 expected to increase the power to detect QTL of lesser effect [41], so we investigated
298 whether epic-QTL has an added benefit of increasing power when a major-effect QTL
299 exists on a fixed chromosome. We found that indeed the majority of peaks in the fixed
300 chromosome VIII experiment had z-scores of greater magnitude than the corresponding
301 peaks in the fixed chromosome I experiment, and that several additional peaks were
302 detected that were not called when chromosome I was fixed (Fig 3). On chromosome
303 XII in particular, only a single peak is obvious in the fixed chromosome I experiment,
304 whereas in the fixed chromosome VIII experiment, two peaks can clearly be
305 differentiated (Fig 3). Taken together, our results for additive QTL demonstrate that
306 epic-QTL has high power, resolution and reproducibility; that copper resistance in the
307 Oak X Wine cross progeny shares at least some underlying mechanisms with other *S.*
308 *cerevisiae* strains; and that removal of a major source of variance can increase power to
309 detect other additive QTL.
310

311 Magnitude epistasis is identified with chromosome VIII but
312 not chromosome I

313 Reciprocal chromosome fixation effectively converts effects that are epistatic with
314 that chromosome into additive effects that can be detected with high power by BSA. In
315 the context of the epic-QTL logistic-regression model, these epistatic effects are
316 identified as significant selection-by-background interactions.

317 We identify seven interactions with chromosome VIII: one each on chromosomes
318 VII, X, XII, XIV, and XV, and two on chromosome XI (Fig 4, S3 Table). The z-score of
319 each interaction peak is less extreme than that of its corresponding additive effect, but
320 not always in the same direction as the additive effect, indicating that there is no
321 consistent interaction effect (such as the Oak chromosome always amplifying Oak
322 alleles' selection effects). We did not identify any interactions at a 5% FDR with
323 chromosome I (Fig 4A), despite observing >10 additive QTL. As chromosome I is the
324 smallest of the *S cerevisiae* chromosomes, it is plausible that there would not be any
325 interactions with the entire chromosome. This result provides evidence that epic-QTL
326 does not generate spurious interactions, and that interactions are specific and not
327 widespread across the genome.
328
329 **Fig 4. Interaction effects indicate magnitude epistasis.** (A) Fixed chromosome I
330 (top) and fixed chromosome VIII (bottom) absolute z-scores for $CuSO_4$ experiments,
331 with trace colors indicating additive (black) and interaction (red) effects.Vertical red lines
332 indicate where an interaction peak has been called, with solid lines indicating the
333 highest peak on a chromosome and dashed lines indicating a second significant peak.
334 (B) Allele frequencies of the Wine allele at the maximum point of each interaction QTL
335 per chromosome (indicated by solid lines in 4A and triangles in 4C), in each population.
336 Oak (O) and Wine (W) fixed chromosome VIII backgrounds are on the horizontal axis,
337 and the allele frequency of the Wine allele is on the vertical axis. Line crossing of
338 selected (blue) and non-selected (gray) would indicate sign epistasis. (C) Comparisons

339 of z-scores at interaction peaks (red triangles) with z-scores at corresponding additive
340 peaks (black triangles).
341
342 The presence of an interaction can indicate different forms of epistasis. One
343 possibility is sign epistasis, which in the case of epic-QTL would mean that changing the
344 parent of the fixed chromosome changes the direction of the QTL effect at the
345 interacting locus. An alternative possibility is magnitude epistasis, in which the QTL
346 effect size at the interacting locus changes but the direction of the effect remains the
347 same. In experimental designs such as standard BSA, where effects at any locus are
348 averaged across a population, sign epistasis obscures phenotypic effect as the effects
349 of allele pairs cancel each other out. Perfect sign epistasis, in which effect magnitude is
350 equal but effect direction is opposite, is therefore impossible to detect by BSA without
351 fixation of one allele in the pair to isolate the effect. In contrast, magnitude epistasis still
352 produces an additive effect, although the effect size will be the average of that of each
353 allele combination. To characterize our interaction QTL as exhibiting sign or magnitude
354 epistasis with the fixed chromosome, we: 1) compared the allele frequencies of the
355 highest points of the interaction peak (Fig 4C), and 2) scanned for loci above the 5%
356 FDR threshold where the interaction z-score was more extreme than its corresponding
357 additive z-score. Sign epistasis would require line-crossing of allele frequencies
358 between parental backgrounds in the selected bulks, which we do not observe at
359 interaction peaks (Fig 4B). We also do not find any significant interaction z-scores that
360 are greater in magnitude than their selection effect (Fig 4C), which would indicate that

361 the interaction obscures the additive effect through averaging. We therefore conclude
362 that epistasis with chromosome VIII is magnitude and not sign epistasis.
363 Prior studies have identified interaction QTL for copper resistance in *S.*
364 *cerevisiae* either by testing for interactions between additive QTL [4] or by barcoding
365 combinations of alleles in natural variants [21,22]. We compared interactions identified
366 with chromosome VIII in our study with those identified in these other studies, which
367 utilized strains other than the Oak and Wine strains used here. We find that there is little
368 overlap between identified loci (S2 Fig). There are, however, consistent additive effects
369 at specific loci such as *CUP1*, and indeed most interactions with chromosome VIII from
370 the other studies did involve the *CUP1* locus. These results suggest that interactions
371 are between specific alleles not necessarily present in all crosses, which could be
372 corroborated with additional epic-QTL experiments with different parental strains.
373 Further evidence that interaction effects are idiosyncratic is that not every
374 additive locus interacts with the fixed chromosome, and there is no correlation in the
375 direction or magnitude of effect of the interaction compared to additive effect (Fig 4C).
376 The majority of interaction peaks (4 of 7) were within 6 kb of the additive peak maxima,
377 indicating that the interactions with chromosome VIII are likely with the same loci that
378 produce additive effects. Of the remaining interaction peaks, two (the one on
379 chromosome VII and the lesser one on XI) overlap with what appear as shoulders of
380 additive peaks, suggesting that multiple QTL occur within that peak, and that the second
381 largest is interacting with chromosome VIII. The peak on chromosome XV might also
382 correspond more with the shoulder of the additive peak. The interaction peak and
383 corresponding additive peak shoulder on chromosome VII are close to the *CUP2* gene,

384 which induces transcription of *CUP1* [35]. *CUP2* could thus be a candidate for allele
385 substitution to confirm the interaction with *CUP1* on chromosome VIII. Overall, the co-
386 occurrences of interaction peaks with additive peaks indicate that interactions occur
387 primarily with loci that have an additive effect, and the lack of interactions at every
388 additive peak, or even the most significant additive peaks, suggests that interactions are
389 specific and idiosyncratic.

390

391 Discussion

392 Identifying epistatic contributions to trait variation presents challenges caused by
393 the combinatorial nature of interactions and their potential to obscure effects of
394 individual alleles. Methods to detect pairwise interaction effects suffer from low
395 statistical power due to the number of pairwise comparisons across the genome to test.
396 High power can be achieved by BSA experiments, but averaging over combinations of
397 alleles precludes analysis of interactions. Because of these challenges, approaches to
398 predicting the effect of genotype often minimize the contribution of epistasis to
399 phenotypic variance, by first (or only) fitting additive effects [9]. However, although the
400 effects of epistasis might be statistically underestimated, specific examples of epistasis
401 have been observed across species and traits such as in tomato size and fruit number
402 [42,43], corn kernel coloration [44], and mouse coat color (39, reviewed by 12). In non-
403 natural variants such as deletion mutations or engineered hypomorphs, interactions
404 have also been quantified; using high-throughput approaches, Costanzo *et.al.* found
405 ~900,000 interactions among 23 million double mutants representing nearly every pair

406 of genes in the yeast genome [24], and Hale *et al.* found that over one quarter of 1721
407 CRISPR-interference perturbations showed growth effects that depend on genetic
408 background [46]. We developed epic-QTL with the aim of bringing the power of a high-
409 throughput, DNA sequencing-based approach to the identification of interactions
410 between natural genetic variants. Specifically, we circumvented the statistical problem
411 of pairwise testing of natural variants by reciprocally fixing a single chromosome from
412 each of two genetic backgrounds in a cross between divergent yeast strains. With the
413 high power afforded by BSA, we observe magnitude epistasis with additive QTL but no
414 evidence of cryptic sign epistasis.

415 We first verified our method by comparing additive QTL identified by epic-QTL,
416 both between experiments with chromosome I or chromosome VIII fixed and between
417 our study and those conducted on copper resistance in other strains. Known drivers of
418 copper resistance, *CUP1* and *FRE1*, were identified as additive QTL in all experiments
419 where the loci were allowed to segregate. Additive peaks colocalized between the
420 experiment with chromosome I fixed and the experiment with chromosome VIII fixed,
421 but on average those identified in the experiment with fixed chromosome VIII were
422 stronger, very likely due to the fixation of a major QTL. In comparison with other studies
423 of copper sulfate resistance, several additive QTL were found in common, but many
424 were not, suggesting strain-specific differences in which alleles are present that impact
425 resistance.

426 The key strength of epic-QTL is identification of interactions with fixed
427 chromosomes at high statistical power. We next compared interactions found by epic-
428 QTL to those identified for copper resistance using different strains, different methods

429 and smaller sample sizes [2,19,21,22], finding that although there is some overlap in
430 regions containing additive QTL, the majority of interactions are not common between
431 studies. This finding speaks to the importance of more high-powered studies of
432 interactions and potentially also suggests that interactions are idiosyncratic in that they
433 are dependent on the specific alleles found in divergent strains. Because we detected
434 more additive than interaction QTL, not every detected additive QTL in our study
435 contained interaction QTL. Moreover, interactions did not necessarily cluster only under
436 the highest additive peaks. This finding further supports that the interactions are
437 idiosyncratic, rather than globally caused by nonlinear transformation of the value of a
438 latent trait with additive genetic architecture [14]. One key overlap with another study to
439 note, however, is *CUP1* as a hub for interactions on chromosome VIII [22]. That
440 interactions occur with chromosome VIII but not chromosome I, and that interactions
441 occur primarily with additive QTL, suggests that our interactions might be with *CUP1*.
442 The logical next step would be to fix the chromosomes found to interact with fixed
443 chromosome VIII, allowing chromosome VIII to segregate, and thereby to identify the
444 interaction partner(s) on this chromosome.

445 The interaction QTL identified here provide evidence of three compelling trends
446 that imply a middle ground between completely idiosyncratic epistasis and highly
447 predictable global epistasis: 1) interaction peaks commonly colocalized with additive
448 peaks, 2) magnitude epistasis was observed whereas sign epistasis was notably
449 absent, and 3) interaction peaks differ between studies and are not driven by strength of
450 an additive peak. Sign epistasis has the potential to completely obscure additive effects,
451 and thus the lack of sign epistasis implies that interactions occur primarily with loci that

452 already have an effect. Precise colocalization of additive and interaction maxima
453 suggest that the additive QTL interacts with the fixed chromosome. These trends
454 corroborate the conclusion by Bloom *et al.* [4] that interactions occur primarily between
455 additive QTL, and they validate the approach of reducing the search space by only
456 looking at interactions between additive QTL as done by Nguyen Ba *et al.* [21].

457 Sign but not magnitude epistasis can influence available evolutionary trajectories
458 by creating valleys between peaks on a fitness landscape [11,13]. Examples of specific
459 reciprocal sign epistasis, for example mutually exclusive adaptive mutations in the
460 *HXT6/7* and *MTH1* genes during experimental evolution under glucose limitation, have
461 been shown to cause fitness valleys [47]. Sign epistasis involving mutations in specific
462 interaction hubs has also been observed [25], but the general prevalence of sign
463 epistasis is yet to be determined. epic-QTL offers an unbiased, powerful method for
464 detecting sign epistasis. The lack of sign epistasis detected here therefore indicates that
465 it is relatively rare, at least for the trait, fixed chromosomes, and parental strains we
466 studied.

467 It will be important to see whether the trends we observed generalize to other
468 fixed chromosomes and other complex traits. A complete set of fixed-chromosome
469 strains would yield an additional benefit of very rapid assessment of the extent to which
470 epistasis impacts variation in a trait, in that a completely additive genetic architecture
471 would mean that the sum of chromosome effects should equal the difference between
472 the parental strains. Such a test only requires chromosome-substituted strains, not
473 segregants from them. When this kind of test was applied in mice and rats to a large

474 number of anatomical and physiological traits, it revealed much evidence for epistasis
475 [48].
476 A widespread lack of sign epistasis would greatly aid in identifying interactions in
477 studies where experimental manipulations of genotypes are not possible. Genome-wide
478 association studies in particular face challenges with respect to the number of subjects
479 relative to the number of possible interactions between markers, and so a variety of
480 methods have been proposed to avoid exhaustively searching all possible pairs of
481 polymorphisms [49]. Prioritizing interactions between additive loci rather than every
482 possible combination could therefore be a principled approach to increase the power to
483 detect interaction effects. Characterizing interaction effects in humans should in turn
484 allow for greater precision in predicting response to medication and susceptibility to
485 disease, as well as facilitate further understanding of the molecular mechanisms of
486 complex traits. In all, our characterization of epistasis not only enhances our
487 understanding of genetic interactions in model organisms but also has implications for
488 improvement of applications in personalized medicine and trait prediction across diverse
489 species.
490

491 # Materials and Methods

492 ## Conditional Chromosome Strain Construction

493 Two divergent haploid yeast strains, one oak tree-derived (NCYC3631, MATα)
494 and one wine barrel-derived (NCYC3591, MATa) [29], were each engineered for
495 chromosome removal from diploids and later selection of haploid progeny. To facilitate
496 crosses, strains were modified by homologous recombination at *URA3*, *HO*, and *MAT*α

497 using standard lithium-acetate-based transformation. *URA3* prototrophy was restored
498 (and *KanMX* removed) in wine-derived strains by insertion of *URA3* sequence amplified
499 from the wine-strain parent (BC187). The positive-selection marker *hph*, which confers
500 resistance to hygromycin, was removed from the *HO* locus of each parental strain to
501 allow the marker's use elsewhere. To remove *hph*, we conducted Delitto Perfetto
502 excision [50] using a cassette that allows positive selection for nourseothricin resistance
503 (*NatR*) and negative selection against HSV-*TK*, which encodes the thymidine kinase
504 from herpes simplex virus and thereby confers sensitivity to the pyrimidine analogue 5-
505 fluorodeoxyuridine (FuDR) [51]. Importantly, two identical sequences (*cyc* terminators)
506 flank this cassette and thereby lead to spontaneous excision of the cassette by
507 homology-based repair [50]. Transformants were selected for presence of *NatR* and
508 checked for loss of *hph*. We then counter-selected using FuDR to select for removal of
509 the cassette and resulting loss of both *NatR* and HSV-*TK*.
510 To select for haploids of one mating type in bulks to be sequenced, we
511 engineered the *MATα* locus to contain the HSV-*TK* negative-selection marker for
512 removal of any cell that is not a mating-type a haploid. *MATα* contains a bidirectional
513 promoter driving the expression of the *α1* and *α2* genes, both of which must be active
514 for the cell to sporulate [52]. The negative-selection marker was inserted upstream of *α1*
515 and its promoter, and the *STE3* promoter (*pSTE3*), which is activated by the
516 transcriptional co-activator encoded by *α1*, was placed upstream of *α2* [53]. Thus, the
517 selection cassette was placed in a way that maintains expression of both *α1* and *α2* in
518 mating-type α haploids and in diploids. As a result, the cells retain the ability to mate
519 with mating-type a cells as haploids and to sporulate as diploids, but both diploids and

520 haploid mating-type α haploids are sensitive to FuDR. For this transformation we used
521 the positive-selection marker *hph*. We transformed a cassette containing MATα
522 homology and the positive- and negative-selection markers into the Oak α strain, and
523 then replaced *hph* with *NatR* using lithium acetate homology-directed transformation,
524 allowing use of *hph* in later transformations.

525 For chromosome elimination by driving transcription through the centromere, we
526 constructed an inducible-promoter cassette by using overlapping PCR to combine the
527 HSV-*TK* and *hph* markers from Alexander *et al.* [51], the *GAL1* promoter (*pGAL1*), and
528 regions homologous to the yeast genome adjacent to the centromere. The centromere-
529 region primers matched the primers used by Reid *et al.* [30] or matched sequences very
530 close nearby. These cassettes were transformed into either chromosome I or
531 chromosome VIII in either the Oak α or Wine *a* strains. All strains are detailed in
532 supplemental data (S4 Table). These haploid strains are referred to as the background
533 (Wine a or Oak α) plus [I] or [VIII] to indicate the chromosome that can be eliminated.

534 Wine a[I] and Oak α were mated to produce diploids, and Wine a and Oak α[I]
535 were mated to produce diploids capable of producing the reciprocal chromosome
536 fixation (Fig 1A). Diploids were selected by ability to grow in both the absence of uracil
537 and the presence of nourseothricin, and ploidy was confirmed by flow cytometry using
538 DNA staining with propidium iodide on the Cytek Aurora. To fix chromosome I, diploids
539 were then plated onto medium containing 2% D-Galactose (and lacking glucose) to
540 induce the *GAL1* promoter's transcription through the centromere of the conditional
541 chromosome. Although we did not use markers to select for the loss of a chromosome,
542 plating on galactose and restreaking from single colonies was effective for yielding

543 chromosome loss. Colonies from the restreaked plate were checked by Sanger
544 sequencing to identify a loss of the conditional chromosome (i.e. by loss of
545 heterozygosity on that chromosome), then grown in liquid media and frozen as clonal
546 aneuploid (2N–1) strains, which we term Oak I or Wine I to indicate the parent of origin
547 of the remaining chromosome I in these otherwise hybrid strains. Populations of ~10^7
548 clonal aneuploids were sporulated using 2% potassium acetate for ~10 days at room
549 temperature (25 °C) to produce approximately $4X10^7$ segregants with identical
550 chromosome I of either Oak or Wine background but segregating parental genotypes at
551 all other loci. To select for haploids above and beyond the MAT*α* selection, spores were
552 vortexed for 10 minutes in 50% diethyl ether to kill unsporulated diploids [54]. Surviving
553 spores were rinsed twice in sterile water, then germinated by incubation in 1 mg/mL
554 Zymolyase (Z100T) for 12 minutes before culturing in each experiment. The process
555 was completed identically for the reciprocal fixations of chromosome VIII.
556

557 ## Concentration Determination for Selection

558 We tested approximate concentrations of copper for selection by growing cells in
559 media of different concentrations for 24 hours (matching the experiment time) and then
560 counting the cells either by automatic cell counter (ThermoFisher Countess™ II) or by
561 manual counting on a hemocytometer. From there, we chose smaller ranges of doses
562 that would provide between 1% and 10% survival. After conducting experiments, cell
563 counts in some experiments were checked by hemocytometer to confirm that
564 experimental treatments were achieving the intended amount of selection.
565

566 ## Bulk Segregant Analysis

567 Pools of segregants with reciprocal fixed chromosomes (Oak I and Wine I, or
568 Oak VIII and Wine VIII) were grown in parallel for 24 hours in either YPD or YPD +
569 copper sulfate at doses determined in each chromosome-fixed bulk population to
570 produce between 1% and 10% survival. The control cultures grown in YPD were
571 seeded at 10% of the starting density for the selected group. Each of the four bulk
572 categories was grown in duplicate. After 24 hours, each of these bulks was harvested
573 by spinning down cells separately and extracting DNA either by phenol-chloroform-
574 isoamyl alcohol extraction and ethanol precipitation [55], or by Qiagen DNeasy Blood
575 and Tissue Extraction Kit 69506.

576

577 ## Sequencing

578 After DNA was harvested, single-end libraries for DNA sequencing were
579 prepared according to Baym *et al.*'s protocol [56] using Illumina kit FC-131-2001 and
580 KAPA HiFi amplification kit KK2612. Fragments were selected to be 200–600 bp by
581 AMPure XP bead cleanup (Fisher NC9959336), and pooled based on concentrations
582 determined by LifeTechnologies Qubit 3.0 and Roche 480 LightCycler qPCR. Libraries
583 were then sequenced on an Illumina NovaSeq 6000, with an average per-bulk depth of
584 ~70X. Reads were aligned to the S288C reference genome R64 using BWA-MEM [57],
585 sorted using PicardTools [58], and then underwent quality control using Genome
586 Analysis Toolkit [59] command *BQSR*. Variants were called using GATK
587 *HaplotypeCaller* [60] as described by Mansfield and Grumet [61].

588

589 ## epic-QTL Analysis

590 VCFs were converted to tables of reads to analyze in R using GATK's
591 *VariantsToTable* function. We first removed all loci with >2 alternate alleles to control for
592 mapping quality issues, then assigned each alternate allele to the corresponding parent
593 based on SNP location from whole genome sequencing of the parent strains [62]. To
594 increase our signal-to-noise ratio and take advantage of the inherent correlation of
595 nearby genomic positions in a single F2 cross, we smoothed the read counts in rolling
596 windows of 200 SNPs using a Gaussian weighted mean.

597 To partition the effects of fixed-chromosome parent of origin, selection, and their
598 interaction, we performed logistic regression on these counts for each smoothed
599 position using the following formula:

600

601 $$\log(\textit{allele odds}) = \beta 0 + \beta 1 \cdot \textit{selection} + \beta 2 \cdot \textit{background} + \beta 3 \cdot (\textit{selection} \times \textit{background}) + \epsilon$$

602

603 where *selection* is the presence or absence of copper sulfate in the culture media,
604 *background* is the parent of origin of the fixed chromosome, and the
605 *selection×background* term captures the dependence on background of the selection
606 effect, i.e. epistasis. We then used the z-scores of each effect to identify additive
607 (*selection*) and epistatic (*selection×background*) QTL. Absent any effects of the fixed
608 chromosome's parent of origin on segregation of the other chromosomes or on growth
609 in the absence of copper sulfate, we do not expect to see a significant background
610 effect. For this reason, we set the contrasts of the selection variable to 0 (copper

611 absent) and 1 (copper present), and for the background variable to –0.5 (Wine) and 0.5
612 (Oak). Outputs of this analysis are available in supplemental data (S1 Table).
613 To establish our statistical threshold for interactions, we conducted permutations
614 of allele frequency ratios by shuffling positions within each parent and replicate in the
615 non-selected bulks. This permutation approach is based on the assumption that, in the
616 absence of selection, there would be no loci associated with the trait. For the
617 permutations, we excluded chromosomes I and VIII from all experiments to remove the
618 effect of the fixed chromosomes, and removed chromosomes III and V, which contained
619 engineered regions not identical in the two parents. We then assigned bulks randomly
620 to these permuted values according to the structure of the original dataset (the same
621 number of replicates in each group) and calculated our selection, background, and
622 interaction effects for each. These effects drawn from the bulks of two different parents
623 form the null distribution of z-scores of interaction effects for each experiment. All
624 analyses employ a false discovery rate threshold of 5%.
625 Peaks of absolute z-score (QTL locations) were called by identifying the
626 maximum points within chromosome segments bounded by chromosome ends or local
627 minima, defined as positions where the local slope of the absolute z-score trace shifted
628 from negative to positive. The local slope was calculated within sliding windows of 700
629 SNPs by linear regression within the window. The highest point in that segment, if
630 above the 5% FDR, was then called as the peak. Additive and interaction peak locations
631 are available in supplemental data (S2 and S3 Tables).

Acknowledgements

This work was supported by National Institutes of Health grant R35GM148344 (to MLS), the NYU Biology Summer Undergraduate Research Program (JKV), and the NYU Graduate School of Arts and Science Dean's Dissertation Fellowship (CB). This work was supported in part through the NYU IT High Performance Computing resources, services, and staff expertise. We acknowledge the Zegar Family Foundation for their generous support. We thank the NYU Center for Genomics and System Biology Genomics Core for their assistance and resources. We thank members and alumni of the Siegal lab for input on the paper and discussion about the project.

References

1. Tsouris A, Fournier T, Friedrich A, Hou J, Dunham MJ, Schacherer J. Species-wide survey of the expressivity and complexity spectrum of traits in yeast. PLOS Genet. 2024;20: e1011119. doi:10.1371/journal.pgen.1011119
2. Bloom JS, Ehrenreich IM, Loo WT, Lite T-LV, Kruglyak L. Finding the sources of missing heritability in a yeast cross. Nature. 2013;494: 234–237. doi:10.1038/nature11867
3. Mackay TFC, Stone EA, Ayroles JF. The genetics of quantitative traits: challenges and prospects. Nat Rev Genet. 2009;10: 565–577. doi:10.1038/nrg2612
4. Bloom JS, Kotenko I, Sadhu MJ, Treusch S, Albert FW, Kruglyak L. Genetic interactions contribute less than additive effects to quantitative trait variation in yeast. Nat Commun. 2015;6: 8712. doi:10.1038/ncomms9712
5. Falconer D, Mackay TFC. Introduction to Quantitative Genetics. IV. Longman Group Ltd;

1996.

6. Lynch M, Walsh B. Genetics and Analysis of Quantitative Traits. Sinauer Associates, Inc;

7. Boye C, Nirmalan S, Ranjbaran A, Luca F. Genotype × environment interactions in gene regulation and complex traits. Nat Genet. 2024;56: 1057–1068. doi:10.1038/s41588-024-01776-w

8. Morgante F, Huang W, Maltecca C, Mackay TFC. Effect of genetic architecture on the prediction accuracy of quantitative traits in samples of unrelated individuals. Heredity. 2018;120: 500–514. doi:10.1038/s41437-017-0043-0

9. Ober U, Huang W, Magwire M, Schlather M, Simianer H, Mackay TFC. Accounting for Genetic Architecture Improves Sequence Based Genomic Prediction for a Drosophila Fitness Trait. 2015. doi:doi.org/10.1371/journal.pone.0126880

10. Mackay TFC, Anholt RRH. Pleiotropy, epistasis and the genetic architecture of quantitative traits. Nat Rev Genet. 2024;25: 639–657. doi:10.1038/s41576-024-00711-3

11. Weinreich DM, Watson RA, Chao L. Perspective: Sign epistasis and genetic constraint on evolutionary trajectories. Evol Int J Org Evol. 2005;59: 1165–1174.

12. Phillips PC. Epistasis—the essential role of gene interactions in the structure and evolution of genetic systems. Nat Rev Genet. 2008;9: 855–867. doi:10.1038/nrg2452

13. Phillips PC, Otto SP, Whitlock MC. Beyond the average: the evolutionary importance of gene interactions and variability of epistatic effects. Epistasis and the Evolutionary Process. Oxford; 2000.

14. Otwinowski J, Plotkin JB. Inferring fitness landscapes by regression produces biased estimates of epistasis. Proc Natl Acad Sci. 2014;111: E2301–E2309. doi:10.1073/pnas.1400849111

15. Kryazhimskiy S, Rice DP, Jerison ER, Desai MM. Microbial evolution. Global epistasis makes adaptation predictable despite sequence-level stochasticity. Science. 2014;344: 1519–1522. doi:10.1126/science.1250939

681 16. Johnson MS, Reddy G, Desai MM. Epistasis and evolution: recent advances and an
682 outlook for prediction. BMC Biol. 2023;21: 120. doi:10.1186/s12915-023-01585-3
683 17. Reddy G, Desai MM. Global epistasis emerges from a generic model of a complex trait.
684 Barkai N, Petrov DA, Crona K, Krug J, editors. eLife. 2021;10: e64740.
685 doi:10.7554/eLife.64740
686 18. Ehrenreich IM, Torabi N, Jia Y, Kent J, Martis S, Shapiro JA, et al. Dissection of genetically
687 complex traits with extremely large pools of yeast segregants. Nature. 2010;464: 1039–
688 1042. doi:10.1038/nature08923
689 19. Ehrenreich IM, Bloom J, Torabi N, Wang X, Jia Y, Kruglyak L. Genetic architecture of
690 highly complex chemical resistance traits across four yeast strains. PLoS Genet. 2012;8:
691 e1002570. doi:10.1371/journal.pgen.1002570
692 20. Nadeau JH, Singer JB, Matin A, Lander ES. Analysing complex genetic traits with
693 chromosome substitution strains. Nat Genet. 2000;24: 221–225. doi:10.1038/73427
694 21. Nguyen Ba AN, Lawrence KR, Rego-Costa A, Gopalakrishnan S, Temko D, Michor F, et
695 al. Barcoded bulk QTL mapping reveals highly polygenic and epistatic architecture of
696 complex traits in yeast. Verstrepen KJ, Barkai N, Verstrepen KJ, editors. eLife. 2022;11:
697 e73983. doi:10.7554/eLife.73983
698 22. Matsui T, Mullis MN, Roy KR, Hale JJ, Schell R, Levy SF, et al. The interplay of additivity,
699 dominance, and epistasis on fitness in a diploid yeast cross. Nat Commun. 2022;13: 1463.
700 doi:10.1038/s41467-022-29111-z
701 23. Michelmore RW, Paran I, Kesseli RV. Identification of markers linked to disease-resistance
702 genes by bulked segregant analysis: a rapid method to detect markers in specific genomic
703 regions by using segregating populations. Proc Natl Acad Sci U S A. 1991;88: 9828–9832.
704 24. Costanzo M, VanderSluis B, Koch EN, Baryshnikova A, Pons C, Tan G, et al. A global
705 interaction network maps a wiring diagram of cellular function. Science. 2016;353:
706 aaf1420. doi:10.1126/science.aaf1420

707 25. Ang RML, Chen S-AA, Kern AF, Xie Y, Fraser HB. Widespread epistasis among beneficial
708 genetic variants revealed by high-throughput genome editing. Cell Genomics. 2023;3:
709 100260. doi:10.1016/j.xgen.2023.100260
710 26. Rehman M, Liu L, Wang Q, Saleem MH, Bashir S, Ullah S, et al. Copper environmental
711 toxicology, recent advances, and future outlook: a review. Environ Sci Pollut Res. 2019;26:
712 18003–18016. doi:10.1007/s11356-019-05073-6
713 27. De Freitas J, Wintz H, Hyoun Kim J, Poynton H, Fox T, Vulpe C. Yeast, a model organism
714 for iron and copper metabolism studies. Biometals. 2003;16: 185–197.
715 doi:10.1023/A:1020771000746
716 28. Valentine JS, Gralla EB. Delivering Copper Inside Yeast and Human Cells. Science.
717 1997;278: 817–818. doi:10.1126/science.278.5339.817
718 29. Cubillos FA, Louis EJ, Liti G. Generation of a large set of genetically tractable haploid and
719 diploid Saccharomyces strains. FEMS Yeast Res. 2009;9: 1217–1225. doi:10.1111/j.1567-
720 1364.2009.00583.x
721 30. Reid RJD, Sunjevaric I, Voth WP, Ciccone S, Du W, Olsen AE, et al. Chromosome-Scale
722 Genetic Mapping Using a Set of 16 Conditionally Stable Saccharomyces cerevisiae
723 Chromosomes. Genetics. 2008;180: 1799–1808. doi:10.1534/genetics.108.087999
724 31. Clowers KJ, Heilberger J, Piotrowski JS, Will JL, Gasch AP. Ecological and Genetic
725 Barriers Differentiate Natural Populations of Saccharomyces cerevisiae. Mol Biol Evol.
726 2015;32: 2317–2327. doi:10.1093/molbev/msv112
727 32. Gerke JP, Chen CTL, Cohen BA. Natural Isolates of Saccharomyces cerevisiae Display
728 Complex Genetic Variation in Sporulation Efficiency. Genetics. 2006;174: 985–997.
729 doi:10.1534/genetics.106.058453
730 33. Magwene PM, Willis JH, Kelly JK. The Statistics of Bulk Segregant Analysis Using Next
731 Generation Sequencing. PLOS Comput Biol. 2011;7: e1002255.
732 doi:10.1371/journal.pcbi.1002255

733 34. She R, Jarosz DF. Mapping Causal Variants with Single-Nucleotide Resolution Reveals
734 Biochemical Drivers of Phenotypic Change. Cell. 2018;172: 478-490.e15.
735 doi:10.1016/j.cell.2017.12.015
736 35. Welch J, Fogel S, Buchman C, Karin M. The CUP2 gene product regulates the expression
737 of the CUP1 gene, coding for yeast metallothionein. EMBO J. 1989;8: 255–260.
738 36. Jungmann J, Reins HA, Lee J, Romeo A, Hassett R, Kosman D, et al. MAC1, a nuclear
739 regulatory protein related to Cu-dependent transcription factors is involved in Cu/Fe
740 utilization and stress resistance in yeast. EMBO J. 1993;12: 5051–5056.
741 doi:10.1002/j.1460-2075.1993.tb06198.x
742 37. Taylor MB, Ehrenreich IM. Higher-order genetic interactions and their contribution to
743 complex traits. Trends Genet. 2015;31: 34–40. doi:10.1016/j.tig.2014.09.001
744 38. Adamo GM, Lotti M, Tamás MJ, Brocca S. Amplification of the CUP1 gene is associated
745 with evolution of copper tolerance in Saccharomyces cerevisiae. Microbiol Read Engl.
746 2012;158: 2325–2335. doi:10.1099/mic.0.058024-0
747 39. Hassett R, Kosman DJ. Evidence for Cu(II) Reduction as a Component of Copper Uptake
748 by *Saccharomyces cerevisiae*(∗). J Biol Chem. 1995;270: 128–134.
749 doi:10.1074/jbc.270.1.128
750 40. Georgatsou E, Alexandraki D. Regulated expression of the Saccharomyces cerevisiae
751 Fre1p/Fre2p Fe/Cu reductase related genes. Yeast Chichester Engl. 1999;15: 573–584.
752 doi:10.1002/(SICI)1097-0061(199905)15:7<573::AID-YEA404>3.0.CO;2-7
753 41. Sinha H, David L, Pascon RC, Clauder-Münster S, Krishnakumar S, Nguyen M, et al.
754 Sequential Elimination of Major-Effect Contributors Identifies Additional Quantitative Trait
755 Loci Conditioning High-Temperature Growth in Yeast. Genetics. 2008;180: 1661–1670.
756 doi:10.1534/genetics.108.092932
757 42. Eshed Y, Zamir D. Less-than-additive epistatic interactions of quantitative trait loci in
758 tomato. Genetics. 1996;143: 1807–1817. doi:10.1093/genetics/143.4.1807

759 43. Aguirre L, Hendelman A, Hutton SF, McCandlish DM, Lippman ZB. Idiosyncratic and dose-
760 dependent epistasis drives variation in tomato fruit size. Science. 2023;382: 315–320.
761 doi:10.1126/science.adi5222
762 44. Ford RH. Inheritance of Kernel Color in Corn: Explanations & Investigations. Am Biol
763 Teach. 2000;62: 181–188. doi:10.2307/4450870
764 45. Bennett DC, Lamoreux ML. The color loci of mice--a genetic century. Pigment Cell Res.
765 2003;16: 333–344. doi:10.1034/j.1600-0749.2003.00067.x
766 46. Hale JJ, Matsui T, Goldstein I, Mullis MN, Roy KR, Ville CN, et al. Genome-scale analysis
767 of interactions between genetic perturbations and natural variation. Nat Commun. 2024;15:
768 4234. doi:10.1038/s41467-024-48626-1
769 47. Kvitek DJ, Sherlock G. Reciprocal Sign Epistasis between Frequently Experimentally
770 Evolved Adaptive Mutations Causes a Rugged Fitness Landscape. PLOS Genet. 2011;7:
771 e1002056. doi:10.1371/journal.pgen.1002056
772 48. Shao H, Burrage LC, Sinasac DS, Hill AE, Ernest SR, O'Brien W, et al. Genetic
773 architecture of complex traits: Large phenotypic effects and pervasive epistasis. Proc Natl
774 Acad Sci. 2008;105: 19910–19914. doi:10.1073/pnas.0810388105
775 49. Van Steen K, Moore JH. How to increase our belief in discovered statistical interactions via
776 large-scale association studies? Hum Genet. 2019;138: 293–305. doi:10.1007/s00439-
777 019-01987-w
778 50. Storici F, Resnick MA. Delitto PerfettoTargeted Mutagenesis in Yeast with
779 Oligonucleotides. In: Setlow JK, editor. Genetic Engineering. Boston, MA: Springer US;
780 2003. pp. 189–207. doi:10.1007/978-1-4615-0073-5_9
781 51. Alexander WG, Doering DT, Hittinger CT. High-Efficiency Genome Editing and Allele
782 Replacement in Prototrophic and Wild Strains of Saccharomyces. Genetics. 2014;198:
783 859–866. doi:10.1534/genetics.114.170118
784 52. Haber JE. Mating-Type Genes and *MAT* Switching in *Saccharomyces cerevisiae*.

785 Genetics. 2012;191: 33–64. doi:10.1534/genetics.111.134577
786 53. Sprague GF, Jensen R, Herskowitz I. Control of yeast cell type by the mating type locus:
787 positive regulation of the alpha-specific STE3 gene by the MAT alpha 1 product. Cell.
788 1983;32: 409–415. doi:10.1016/0092-8674(83)90460-9
789 54. Dawes IW, Hardie ID. Selective killing of vegetative cells in sporulated yeast cultures by
790 exposure to diethyl ether. Mol Gen Genet MGG. 1974;131: 281–289.
791 doi:10.1007/BF00264859
792 55. Green MR, Sambrook J. Isolation and Quantification of DNA. Cold Spring Harb Protoc.
793 2018;2018. doi:10.1101/pdb.top093336
794 56. Baym M, Kryazhimskiy S, Lieberman TD, Chung H, Desai MM, Kishony R. Inexpensive
795 Multiplexed Library Preparation for Megabase-Sized Genomes. PLOS ONE. 2015;10:
796 e0128036. doi:10.1371/journal.pone.0128036
797 57. Li H, Durbin R. Fast and accurate long-read alignment with Burrows–Wheeler transform.
798 Bioinformatics. 2010;26: 589–595. doi:10.1093/bioinformatics/btp698
799 58. Picard Tools - By Broad Institute. [cited 26 Sep 2024]. Available:
800 http://broadinstitute.github.io/picard/
801 59. Van Der Auwera GA, Carneiro MO, Hartl C, Poplin R, Del Angel G, Levy-Moonshine A, et
802 al. From FastQ Data to High-Confidence Variant Calls: The Genome Analysis Toolkit Best
803 Practices Pipeline. Curr Protoc Bioinforma. 2013;43. doi:10.1002/0471250953.bi1110s43
804 60. Poplin R, Ruano-Rubio V, DePristo MA, Fennell TJ, Carneiro MO, Van Der Auwera GA, et
805 al. Scaling accurate genetic variant discovery to tens of thousands of samples. 2017.
806 doi:10.1101/201178
807 61. Mansfeld BN, Grumet R. QTLseqr: An R Package for Bulk Segregant Analysis with Next-
808 Generation Sequencing. Plant Genome. 2018;11. doi:10.3835/plantgenome2018.01.0006
809 62. Ziv N, Shuster BM, Siegal ML, Gresham D. Resolving the Complex Genetic Basis of
810 Phenotypic Variation and Variability of Cellular Growth. Genetics. 2017;206: 1645–1657.

doi:10.1534/genetics.116.195180

Supporting information captions

S1 Fig. Survival percentage by strain in CuSO4. Boxplots of survival percentages of Oak (NCYC3631) and Wine (NCYC3591) haploid strains at different concentrations of copper sulfate are shown. Replicate experiments carried out on different dates are represented by different shapes.

S2 Fig. Comparison with copper sulfate interaction peaks from previous studies. Interactions with chromosome VIII identified in our study (shown in black trace of the absolute z-score by genome position) are compared with interaction QTL involving chromosome VIII identified in other copper-resistance studies, which used both different experimental designs and different strains. Beneath the trace from this study, NB (magenta) indicates interaction QTL as identified by Nguyen Ba et al [21], M (turquoise) represents interaction hotspots between strains from Matsui et al. [22], and B (dark blue) represents interaction QTL as identified by Bloom et al [4]. Red vertical lines indicate significant peaks called in our study. *CUP1* is indicated by the vertical light blue dotted line on Chromosome VIII.

S1 Table. Logistic regression output. Direct output from logistic regression on sequencing data for each divergent SNP that passes quality filters (see github for code). Each row (numbered in column A) records the effect term in the model (Background, Bulk, Interaction, or intercept (column B, “label”); the chromosome fixed in the

834 experiment (column C, “chr”); the chromosome containing the SNP (column D,
835 “CHROM”); the chromosomal position of the SNP (column E, “POS”); the z-score of that
836 SNP in that experiment and for the specified effect (column F, “zscore”); and the
837 threshold value for a 5% FDR for the specified effect and experiment (column G, “q5”).
838
839 **S2 Table. Additive-effect peaks**. Peaks called for the Bulk effect. Each row records
840 the chromosome fixed in the experiment (column A, “CSS”), the location of the peak
841 SNP as its chromosome (column B, “CHROM”) and chromosomal position (column C,
842 “POS”), and the z-score of the peak SNP (column D, “zscore”).
843
844 **S3 Table. Interaction peaks**. Peaks called for the Interaction effect. Columns are as in
845 S2 Table.
846
847 **S4 Table. Yeast strains constructed and used in experiments**. Backgrounds,
848 genotypes, and aliases of all strains used, including those representing intermediate
849 steps to construct strains for epic-QTL experiments. MLS.CB refers to strains made in
850 this study; NCYC refers to strains from the NCYC collection [29].

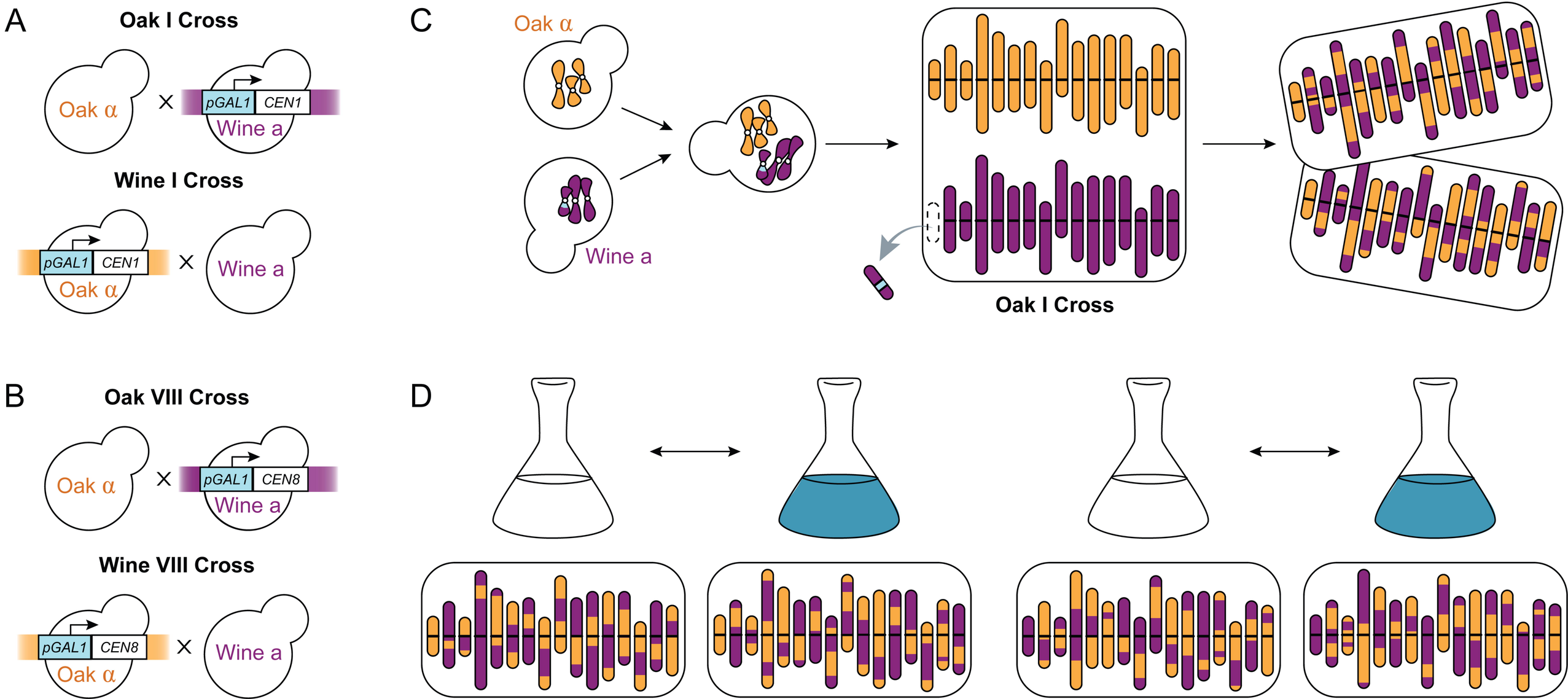
A
Oak I Cross
Oak α
×
pGAL1
CEN1
Wine a
Wine I Cross
pGAL1
CEN1
Oak α
×
Wine a
B
Oak VIII Cross
Oak α
×
pGAL1
CEN8
Wine a
Wine VIII Cross
pGAL1
CEN8
Oak α
×
Wine a
C
Oak α
Wine a
Oak I Cross
D

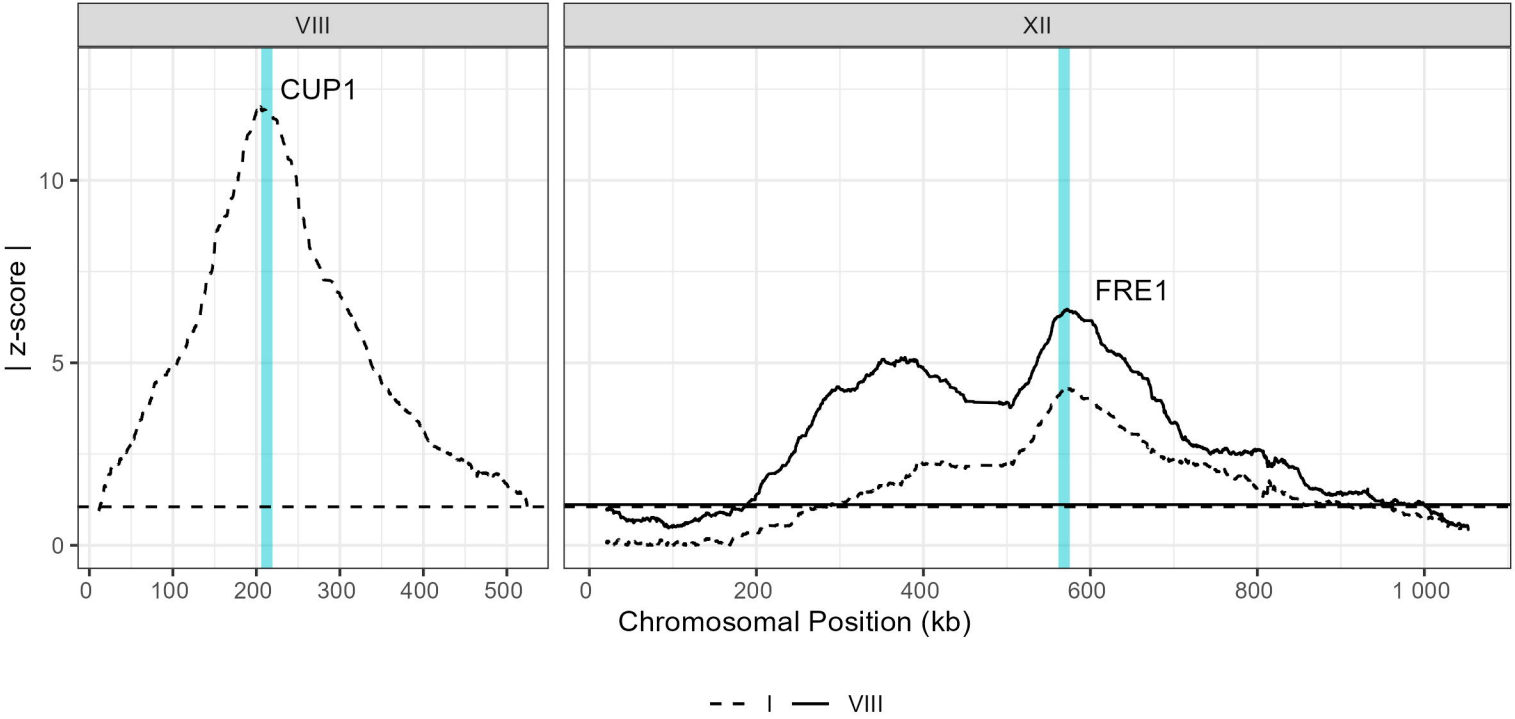
VIII
XII
CUP1
FRE1
| z-score |
10
5
0
0
100
200
300
400
500
0
200
400
600
800
1 000
Chromosomal Position (kb)
I
VIII

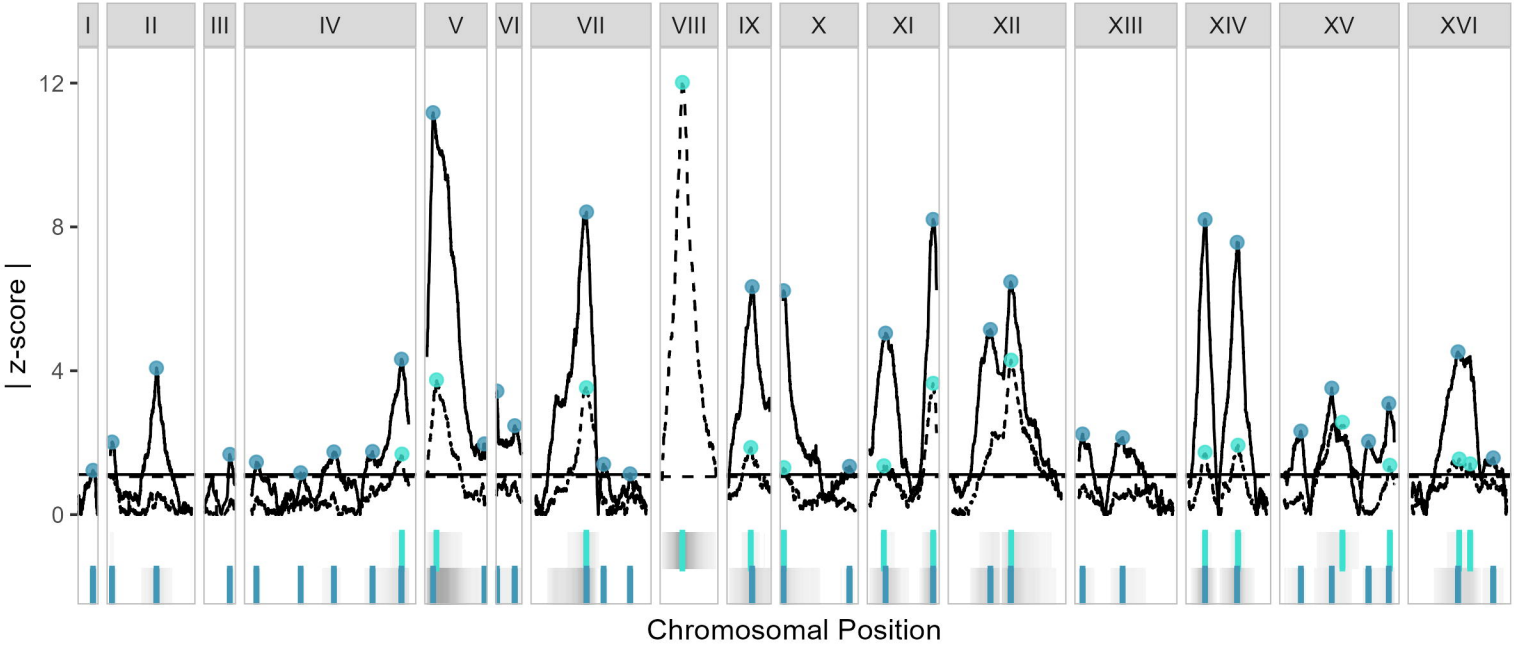
I
II
III
IV
V
VI
VII
VIII
IX
X
XI
XII
XIII
XIV
XV
XVI
12
8
4
0
| z-score |
Chromosomal Position

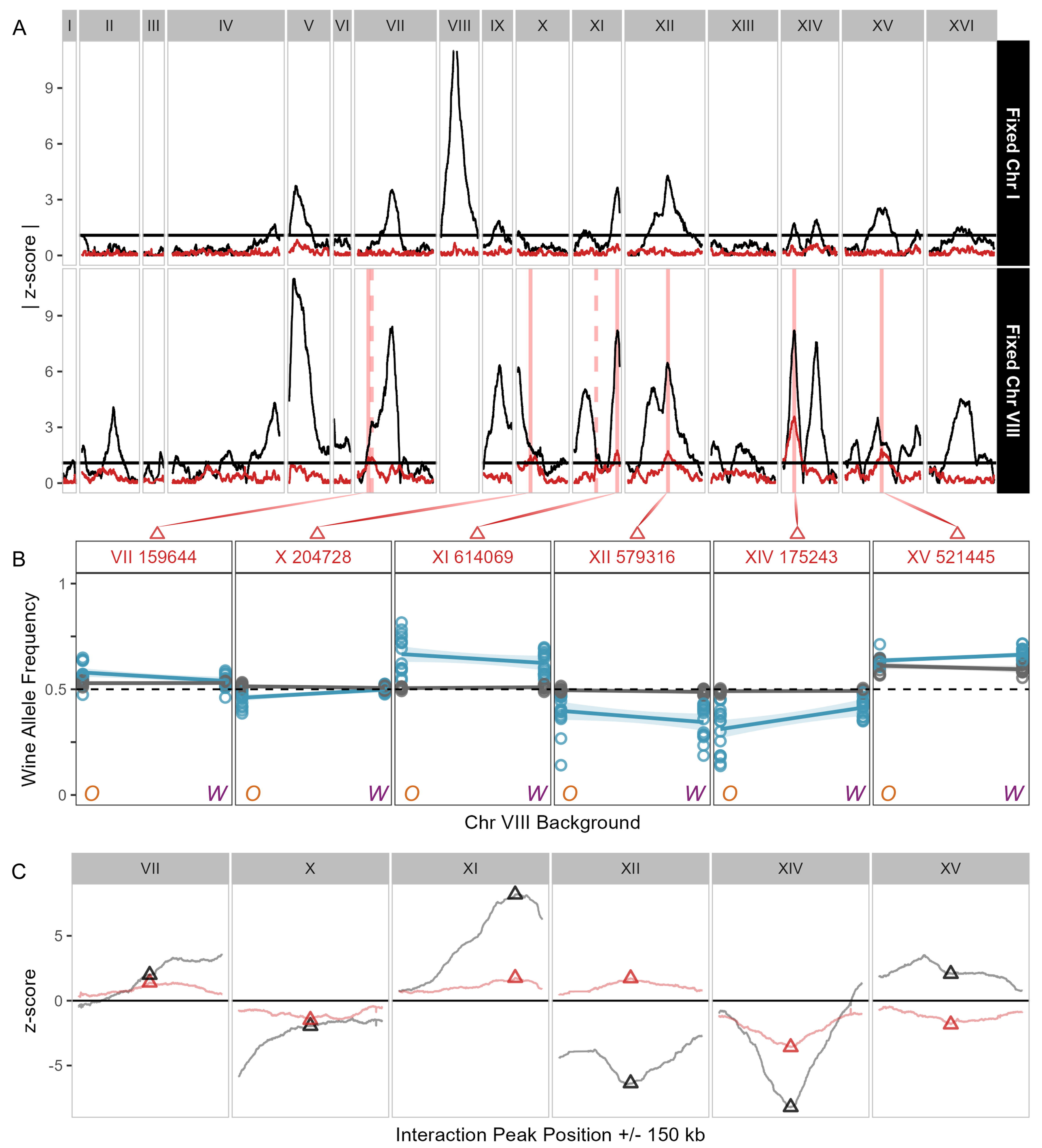
A
I
II
III
IV
V
VI
VII
VIII
IX
X
XI
XII
XIII
XIV
XV
XVI
| z-score |
Fixed Chr I
Fixed Chr VIII
B
VII 159644
X 204728
XI 614069
XII 579316
XIV 175243
XV 521445
Wine Allele Frequency
O
W
Chr VIII Background
C
VII
X
XI
XII
XIV
XV
z-score
Interaction Peak Position +/- 150 kb